^{64}Cu-Labeled Tetrameric and Octameric RGD Peptides for Small-Animal PET of Tumor $\alpha_v\beta_3$ Integrin Expression

Zi-bo Li, Weibo Cai, Qizhen Cao, Kai Chen, Zhanhong Wu, Lina He, and Xiaoyuan Chen

Molecular Imaging Program at Stanford, Department of Radiology and Bio-X Program, Stanford University School of Medicine, Stanford, California

Integrin $\alpha_v\beta_3$ plays a critical role in tumor angiogenesis and metastasis. Suitably radiolabeled cyclic arginine-glycine-aspartic (RGD) peptides can be used for noninvasive imaging of $\alpha_v\beta_3$ expression and targeted radionuclide therapy. In this study, we developed ^{64}Cu-labeled multimeric RGD peptides, E{E[c(RGDyK)]$_2$}$_2$ (RGD tetramer) and E(E{E[c(RGDyK)]$_2$}$_2$)$_2$ (RGD octamer), for PET imaging of tumor integrin $\alpha_v\beta_3$ expression. **Methods:** Both RGD tetramer and RGD octamer were synthesized with glutamate as the linker. After conjugation with 1,4,7,10-tetra-azacyclododecane-*N,N′,N″,N‴*-tetraacetic acid (DOTA), the peptides were labeled with ^{64}Cu for biodistribution and small-animal PET imaging studies (U87MG human glioblastoma xenograft model and c-neu oncomouse model). A cell adhesion assay, a cell-binding assay, receptor blocking experiments, and immunohistochemistry were also performed to evaluate the $\alpha_v\beta_3$-binding affinity/specificity of the RGD peptide-based conjugates in vitro and in vivo. **Results:** RGD octamer had significantly higher integrin $\alpha_v\beta_3$-binding affinity and specificity than RGD tetramer analog (inhibitory concentration of 50% was 10 nM for octamer vs. 35 nM for tetramer). ^{64}Cu-DOTA-RGD octamer had higher tumor uptake and longer tumor retention than ^{64}Cu-DOTA-RGD tetramer in both tumor models tested. The integrin $\alpha_v\beta_3$ specificity of both tracers was confirmed by successful receptor-blocking experiments. The high uptake and slow clearance of ^{64}Cu-DOTA-RGD octamer in the kidneys was attributed mainly to the integrin positivity of the kidneys, significantly higher integrin $\alpha_v\beta_3$-binding affinity, and the larger molecular size of the octamer, as compared with the other RGD analogs. **Conclusion:** Polyvalency has a profound effect on the receptor-binding affinity and in vivo kinetics of radiolabeled RGD multimers. The information obtained here may guide the future development of RGD peptide-based imaging and internal radiotherapeutic agents targeting integrin $\alpha_v\beta_3$.

Key Words: integrin $\alpha_v\beta_3$; RGD multimer; tumor angiogenesis; positron emission tomography (PET); ^{64}Cu

J Nucl Med 2007; 48:1162–1171
DOI: 10.2967/jnumed.107.039859

Angiogenesis is an invasive process characterized by endothelial cell proliferation, modulation of the extracellular matrix, and cell adhesion/migration (*1*). Angiogenesis has been shown to be required for both tumor growth and metastasis (*2–4*). Among many angiogenic factors, the cell adhesion molecule integrin is an important mediator in many tumor types, including glioma and breast cancer (*5,6*). Integrin $\alpha_v\beta_3$, in particular, was found to be necessary for the formation, survival, and maturation of new blood vessels (*7,8*), and its expression correlates with tumor grade and histologic type in several cancer types (*9*). Antagonists of $\alpha_v\beta_3$ integrin have been shown to inhibit tumor angiogenesis and metastasis (*10,11*). Molecular imaging of $\alpha_v\beta_3$ integrin expression during tumor angiogenesis will play a pivotal role in visualizing and quantifying $\alpha_v\beta_3$ integrin expression level, in more appropriately selecting patients considered for anti-integrin $\alpha_v\beta_3$ treatment, and in monitoring treatment efficacy in $\alpha_v\beta_3$-positive patients.

In the past decade or so, integrin $\alpha_v\beta_3$ has been found to serve as a receptor for a variety of proteins and small peptides with the exposed arginine-glycine-aspartic (RGD) sequence (*1,7–11*). Significant progress has also been made in the development of radiolabeled RGD-containing peptides to target integrin $\alpha_v\beta_3$ overexpressed in various tumors (*12–17*). We and others have found that multimeric RGD peptides can significantly enhance the affinity of the receptor–ligand interaction through the polyvalency effect (*13,18–23*). Recent reports on the use of multimeric RGD peptides for ligand endocytosis, imaging of angiogenesis, and targeting of tumors have demonstrated that polyvalency is an efficient strategy for discovering and developing novel RGD-based compounds with better targeting capability and higher cellular uptake because of the increased integrin recognition ability (*24–27*). Although we and others have already successfully developed dimeric and tetrameric RGD peptides that are suitable for diagnosis, further improvement on tumor retention and absolute uptake is still needed before they may be applied for effective peptide receptor radiotherapy.

Received Jan. 21, 2007; revision accepted Mar. 20, 2007.
For correspondence or reprints contact: Xiaoyuan Chen, PhD, Molecular Imaging Program at Stanford, Department of Radiology and Bio-X Program, Stanford University School of Medicine, 1201 Welch Rd., P095, Stanford, CA 94305-5484.
E-mail: shawchen@stanford.edu

Herein, we report the design, synthesis, and evaluation of the new tetrameric and octameric RGD peptides based on the polyvalency principle. These multimeric RGD peptides were constructed on the c(RGDyK) motif with glutamate as the branching unit. They were conjugated with the macrocylic chelator 1,4,7,10-tetraazacyclododecane-*N,N′,N″,N‴*-tetraacetic acid (DOTA) and labeled with ^{64}Cu for small-animal PET imaging of integrin $\alpha_v\beta_3$ expression in both the c-neu oncomouse model (murine mammary carcinoma) and a subcutaneous U87MG xenograft (human glioblastoma) model. The aim of this study was to investigate the $\alpha_v\beta_3$-targeting characteristics of ^{64}Cu-DOTA-RGD multimers in vitro and in vivo, thereby providing information for the future design of radiolabeled RGD peptide agents based on the polyvalency effect.

MATERIALS AND METHODS

All commercially available reagents were used without further purification. DOTA was purchased from Macrocyclics, Inc. Dicyclcohexylcarbodiimide, 1-ethyl-3-[3-(dimethylamino)propyl]-carbodiimide (EDC), *N*-hydroxysulfonosuccinimide (SNHS), trifluoroacetic acid (TFA), and Chelex 100 resin (50-100 mesh) were purchased from Aldrich. Water and all buffers were passed through a Chelex 100 column (1 × 15 cm) before radiolabeling. Reversed-phase extraction C-18 Sep-Pak cartridges were obtained from Waters. The syringe filter and polyethersulfone membranes (pore size, 0.2 μm; diameter, 13 mm) were obtained from Nalge Nunc International. ^{125}I-Echistatin (specific activity, 74,000 GBq/mmol) was purchased from GE Healthcare. Female athymic nude mice (4–6 wk old) were supplied from Harlan. ^{64}Cu (half-life, 12.7 h; β^+, 17.4%; β^-, 30%) was obtained by using the ^{64}Ni(p,n)^{64}Cu nuclear reaction from University of Wisconsin–Madison. The dimeric RGD peptide E[c(RGDyK)]$_2$ was synthesized by Peptides International, Inc. Analytic and semipreparative reversed-phase high-performance liquid chromatography (HPLC) was performed on a Dionex 680 chromatography system with a UVD 170U absorbance detector and model 105S single-channel radiation detector (Carroll and Ramsey Associates). DOTA-conjugated peptides and ^{64}Cu-labeled peptides were isolated using a Vydac protein and peptide column (218TP510; 5 μm, 250 × 10 mm). The flow rate was 3 mL/min for semipreparative HPLC, with the mobile phase starting from 95% solvent A (0.1% TFA in water) and 5% solvent B (0.1% TFA in acetonitrile) (0–2 min) to 35% solvent A and 65% solvent B at 32 min. The analytic HPLC was performed with the same gradient system but with a Vydac 218TP54 column (5 μm, 250 × 4.6 mm) at a flow rate of 1 mL/min. The ultraviolet absorbance was monitored at 218 nm.

Preparation of E{E[c(RGDyK)]$_2$}$_2$ (RGD Tetramer) and E(E{E[c(RGDyK)]$_2$}$_2$)$_2$ (RGD Octamer)

The Boc-protected glutamic acid activated ester Boc-E(OSu)$_2$ was prepared as previously reported (*20*). To a solution of Boc-E(OSu)$_2$ (4.4 mg, 0.01 mmol) in 1 mL of anhydrous *N,N*-dimethylformamide, 3 equivalents of RGD dimer (E[c(RGDyK)]$_2$, 40 mg, 0.03 mmol) or RGD tetramer were added. The pH of the resulting mixture was adjusted to 8.5–9.0 with diisopropylethyl amine. After stirring at room temperature overnight, the desired product, Boc-RGD tetramer or Boc-RGD octamer, was isolated by preparative HPLC. The Boc group was then removed by anhydrous TFA, and the crude product was again purified by HPLC. Seventeen milligrams of RGD tetramer were obtained as a white powder with 58% overall yield (analytic HPLC retention time R_t, 13.3 min). Matrix-assisted laser desorption/ionization (MALDI) time-of-flight (TOF) mass spectrometry (MS): m/z 2,811.0 for $[MH]^+$ ($C_{123}H_{180}N_{39}O_{38}$, calculated molecular weight 2,811.3). RGD octamer was obtained in 46% overall yield (analytic HPLC R_t, 14.3 min). MALDI-TOF-MS: m/z 5,735.5 for $[MH]^+$ ($C_{251}H_{364}N_{79}O_{78}$, calculated molecular weight 5,734.7).

DOTA Conjugation and Radiolabeling

DOTA was activated and conjugated to RGD multimers as reported earlier (*20*). DOTA-RGD multimers were purified by semipreparative HPLC. Details of the ^{64}Cu-labeling procedure were reported earlier (*20*). In brief, 20 μL of $^{64}CuCl_2$ (74 MBq in 0.1N HCl) were diluted in 400 μL of 0.1 mol/L sodium acetate buffer (pH 6.5) and added to the DOTA-RGD multimer (a 1 mg/mL solution of peptide was made and separated into aliquots; 5 μg of DOTA-RGD tetramer and 10 μg of DOTA-RGD octamer per 37 MBq of ^{64}Cu were used for the labeling). The reaction mixture was incubated for 1 h at 50°C. ^{64}Cu-DOTA-RGD tetramer/octamer was then purified by semipreparative HPLC, and the radioactive peak containing the desired product was collected. After removal of the solvent by rotary evaporation, the residue was reconstituted in 800 μL of phosphate-buffered saline and passed through a 0.22-μm syringe filter for in vivo animal experiments.

Cell Adhesion Assay

Ninety-six–well plates were coated with 2 μg of fibronectin or vitronectin (Sigma-Aldrich) per milliliter in phosphate-buffered saline at 4°C overnight and treated with 2% bovine serum albumin for 1 h at 37°C. U87MG cells (human glioblastoma, American Type Culture Collection; 2×10^5 cells/mL) with various concentrations of RGD multimers (50, 200, and 800 nM) in 100 μL of serum-free Dulbecco's modified Eagle's medium containing 0.1% bovine serum albumin were incubated for 20 min at 37°C. The resulting mixture was added to the plates and incubated for 1 h at 37°C. Plates treated with only bovine serum albumin were used as a negative control. After removal of the medium by aspiration, 0.04% crystal violet solution was added and incubated for 10 min at room temperature. The wells were washed 3 times with phosphate-buffered saline, and 20 μL of Triton X-100 (Union Carbide) were added for permeabilization. Distilled water (80 μL) was then added, and the number of adherent cells was assessed with a microplate reader (Tecan; measurement wavelength, 550 nm; reference wavelength, 630 nm).

Cell Integrin Receptor-Binding Assay

The in vitro integrin-binding affinity and specificity of RGD multimers and DOTA-RGD multimers were assessed via competitive cell-binding assays using ^{125}I-echistatin as the integrin $\alpha_v\beta_3$-specific radioligand (*20*). The best-fit 50% inhibitory concentration (IC_{50}) values for U87MG cells were calculated by fitting the data with nonlinear regression using GraphPad Prism with a 450- to 600-keV energy window (GraphPad Software, Inc.). Experiments were performed on triplicate samples.

Animal Models

Animal procedures were performed according to a protocol approved by Stanford University Institutional Animal Care and Use Committee. The U87MG xenograft model was generated by subcutaneous injection of 1×10^7 U87MG cells (integrin $\alpha_v\beta_3$-positive) into the front left flank of female athymic nude

mice. Three to 4 wk after inoculation (tumor volume, 100–400 mm^3), the mice (about 9–10 wk old, with a body weight of 20–25 g) were used for biodistribution and PET studies. The c-neu oncomouse (integrin $\alpha_v\beta_3$-positive; Charles River Laboratories) is a spontaneous tumor-bearing model that carries an activated c-neu oncogene driven by a mouse mammary tumor virus promoter. Transgenic mice uniformly expressing the mouse mammary tumor virus/c-neu gene develop mammary adenocarcinomas (4–8 mo postpartum) that involve the entire epithelium in each gland. The animals were scanned at 7 mo old at about a 20-g body weight, and the tumors were on both sides of the body (*28*).

Biodistribution Studies

Female nude mice received a 0.74- to 1.11-MBq injection of ^{64}Cu-DOTA-RGD tetramer or ^{64}Cu-DOTA-RGD octamer to evaluate the distribution of these tracers in the major organs of mice (*20*). A blocking experiment was also performed by coinjecting radiotracer with a saturating dose of c(RGDyK) (10 mg/kg of mouse body weight). All mice were sacrificed and dissected at 20 h after injection of the tracer. Blood, U87MG tumor, major organs, and tissues were collected and weighed wet. The radioactivity in the tissue was measured using a γ-counter (Packard). The results were presented as percentage injected dose per gram of tissue (%ID/g). For each mouse, the radioactivity of the tissue samples was calibrated against a known aliquot of the injectate and normalized to a body mass of 20 g. Values were expressed as mean ± SD for a group of 3 animals.

Small-Animal PET Studies

PET scans and image analysis were performed using a rodent scanner (microPET R4; Siemens Medical Solutions) as previously reported (*13,20*). About 9.3 MBq of ^{64}Cu-DOTA-RGD multimer were intravenously injected into each mouse under isoflurane anesthesia. Five-minute static scans were acquired at 30 min and at 1, 2, 6, and 20 h after injection. The images were reconstructed by a 2-dimensional ordered-subsets expectation maximum algorithm, and no correction was applied for attenuation or scatter. For each PET scan, regions of interest were drawn over the tumor, normal tissue, and major organs on decay-corrected whole-body coronal images. The radioactivity concentration (accumulation) within a tumor was obtained from the maximum value within the multiple regions of interest and then converted to %ID/g (*20*). For a receptor-blocking experiment, mice bearing U87MG tumors on the front left flank were scanned (5-min static) after coinjection of 9.3 MBq of ^{64}Cu-DOTA-RGD multimer and 10 mg of c(RGDyK) per kilogram.

Statistical Analysis

Quantitative data were expressed as mean ± SD. Means were compared using 1-way ANOVA and the Student *t* test. *P* values of less than 0.05 were considered statistically significant.

RESULTS

Chemistry and Radiochemistry

RGD tetramer and RGD octamer were synthesized through an active ester method by coupling Boc-E$(OSu)_2$ with RGD dimer/tetramer followed by TFA deprotection. In aqueous solution, DOTA was activated with EDC/SNHS, and the resulting DOTA-sulfosuccinimide ester was conjugated with RGD tetramer/octamer to yield DOTA-RGD tetramer and DOTA-RGD octamer (Fig. 1). DOTA-RGD tetramer was synthesized in 70% yield (analytic HPLC R_t, 14.5 min). MALDI-TOF-MS: m/z 3,199.0 for $[MH]^+$ ($C_{140}H_{207}N_{42}O_{45}$, calculated molecular weight 3,198.4). DOTA-RGD octamer was produced in 67% (analytic HPLC R_t, 14.5 min). MALDI-TOF-MS: m/z 6,122.3 for $[MH]^+$ ($C_{267}H_{390}N_{83}O_{85}$, calculated molecular weight 6,121.9). On the analytic HPLC, no significant difference in retention time was observed between ^{64}Cu-DOTA-RGD multimer and DOTA-RGD multimer. ^{64}Cu was labeled in 80%–90% decay-corrected yield with radiochemical purity of more than 98%. The specific activity of ^{64}Cu-DOTA-RGD tetramer and ^{64}Cu-DOTA-RGD octamer was about 23 MBq/nmol (0.62 Ci/μmol).

Cell Adhesion Assay

The effect of RGD multimers on U87MG cell adhesion ability was investigated. Both fibronectin and vitronectin are ligands for integrin $\alpha_v\beta_3$. Fibronectin binds to several other integrins besides $\alpha_v\beta_3$, whereas vitronectin is integrin $\alpha_v\beta_3$–specific (*29,30*). For fibronectin-coated plates, no significant difference in U87MG cell adhesion ability was observed in the presence of RGD multimers at the tested concentration range (Fig. 2A). For vitronectin-coated plates, RGD multimers inhibited cell adhesion in a concentration-dependent manner. The ability of different RGD peptides to inhibit cell adhesion at the same concentration followed the order of monomer < dimer < tetramer < octamer (Fig. 2B). The calculated IC_{50} values for RGD monomer, dimer, tetramer, and octamer were $(2.7 \pm 0.7) \times 10^{-6}$, $(7.0 \pm 1.0) \times 10^{-7}$, $(3.2 \pm 0.9) \times 10^{-7}$, and $(1.1 \pm 0.2) \times 10^{-7}$ mol/L, respectively (Supplemental Fig. 1; supplemental figures are available online only at http://jnm.snmjournals.org). RGD octamer was 3 times as effective as RGD tetramer and 27 times as effective as RGD monomer.

Cell-Binding Assay

We compared the receptor-binding affinity of RGD dimer, tetramer, and octamer; DOTA-RGD tetramer; and DOTA-RGD octamer using a competitive cell-binding assay (Fig. 2C). All peptides inhibited the binding of ^{125}I-echistatin to $\alpha_v\beta_3$ integrin-positive U87MG cells in a dose-dependent manner. The IC_{50} values for RGD dimer, tetramer, and octamer were $(1.0 \pm 0.1) \times 10^{-7}$, $(3.5 \pm 0.3) \times 10^{-8}$, and $(1.0 \pm 0.2) \times 10^{-8}$ mol/L, respectively ($n = 3$). DOTA conjugation had a minimal effect on the receptor-binding avidity, and the IC_{50} values for DOTA-RGD tetramer and DOTA-RGD octamer were $(2.8 \pm 0.4) \times 10^{-8}$ and $(1.1 \pm 0.2) \times 10^{-8}$ mol/L, respectively. The cell-binding assay demonstrated that RGD tetramer had about 3-fold higher integrin $\alpha_v\beta_3$ avidity than RGD dimer, and RGD octamer further increased the integrin avidity by another 3-fold (attributed to the polyvalency effect). The IC_{50} values measured from such a cell-binding assay are always lower than those obtained from purified $\alpha_v\beta_3$ integrin protein fixed on a solid matrix (e.g., an ELISA and solid-phase receptor-binding assay) (*31*).

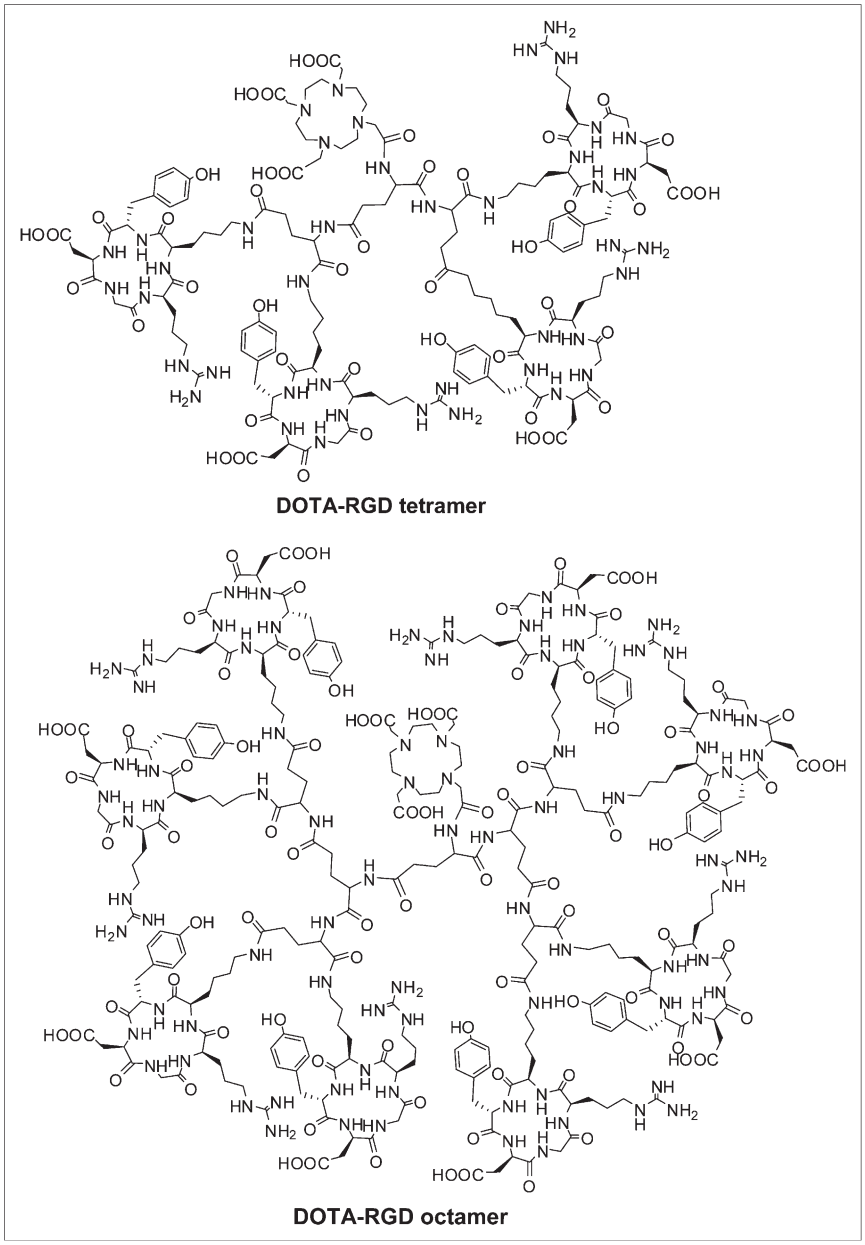

FIGURE 1. Chemical structures of DOTA-RGD tetramer and DOTA-RGD octamer.

PET Imaging of U87MG Tumor-Bearing Mice and c-Neu Oncomice

The tumor-targeting efficacy of ^{64}Cu-DOTA-RGD tetramer and ^{64}Cu-DOTA-RGD octamer in U87MG tumor-bearing nude mice ($n = 3$ per tracer) was evaluated by multiple time-point static PET scans. Representative decay-corrected coronal images at different times after injection are shown in Figure 3A. The U87MG tumors were clearly visualized with high tumor-to-background contrast for both tracers. The uptake of ^{64}Cu-DOTA-RGD tetramer in U87MG tumors was rapid and high, reaching 10.3 ± 1.6, 9.6 ± 1.4, 8.6 ± 1.0, 7.7 ± 1.6, and 6.4 ± 0.7 %ID/g at 0.5, 1, 2, 6, and 20 h after injection, respectively (Fig. 4A). The activity accumulation of ^{64}Cu-DOTA-E$\{$E[c(RGDyK)]$_2\}_2$ (the D-Tyr analog) in U87MG tumor was slightly higher than of ^{64}Cu-DOTA-E$\{$E[c(RGDfK)]$_2\}_2$ (the D-Phe analog) (*20*), and no significant difference in liver and kidney uptake was observed between D-Tyr and D-Phe RGD tetramer analogs, similar to previous reports for RGD dimers (*32*).

Uptake of ^{64}Cu-DOTA-RGD octamer was higher than of ^{64}Cu-DOTA-RGD tetramer in U87MG tumors at all time points examined, reaching 11.7 ± 0.7, 10.6 ± 0.7, 10.6 ± 0.3, 10.5 ± 0.7, and 10.3 ± 1.0 %ID/g at 0.5, 1, 2, 6, and 20 h after injection, respectively (Fig. 4A). Washout from the tumor during the experimental time span was minimal (20 h). Activity accumulation in the liver, kidneys, and muscle is also shown in Figure 4A. Uptake of the 2 tracers in the liver and muscle was similar, whereas uptake in kidney of ^{64}Cu-DOTA-RGD octamer was much higher than of ^{64}Cu-DOTA-RGD tetramer. Representative coronal images of U87MG

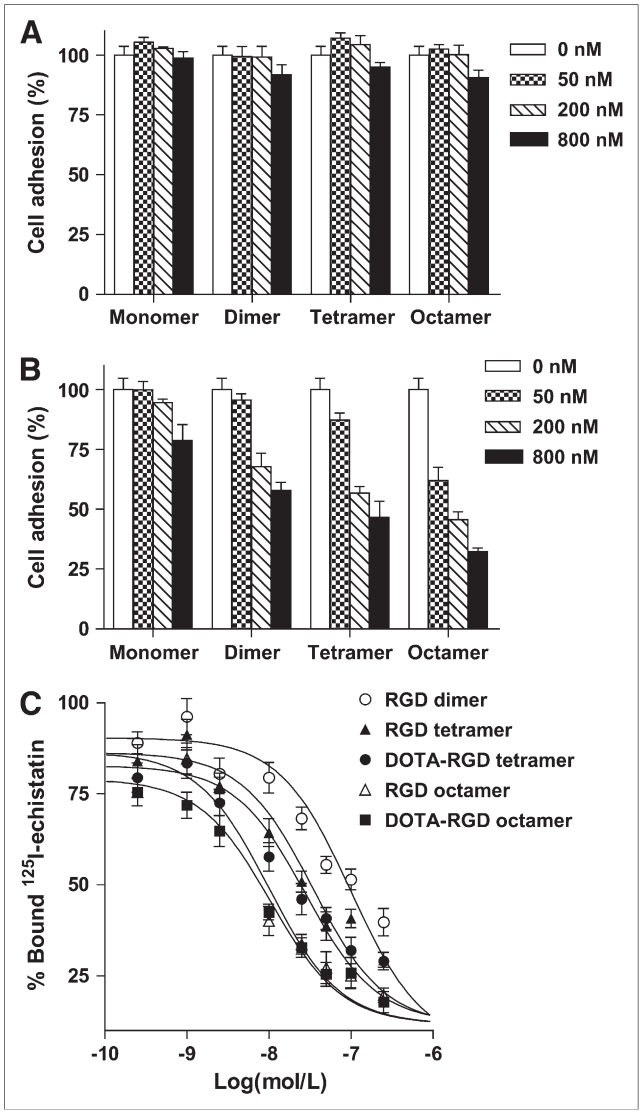

FIGURE 2. In vitro cell adhesion assay and cell-binding assay using U87MG human glioblastoma cells. (A) Cell adhesion assay of RGD monomer, dimer, tetramer, and octamer on fibronectin-coated plates (n = 4, mean ± SD). (B) Cell adhesion assay of RGD monomer, dimer, tetramer, and octamer on vitronectin-coated plates (n = 4, mean ± SD). (C) Inhibition of ^{125}I-echistatin (integrin $\alpha_v\beta_3$–specific) binding to $\alpha_v\beta_3$ integrin on U87MG cells by RGD dimer, tetramer, octamer, DOTA-RGD tetramer, and DOTA-RGD octamer (n = 3, mean ± SD).

tumor–bearing mice with and without coinjection of a blocking dose of c(RGDyK) (10 mg/kg) are shown in Figure 3B. Tracer uptake in the U87MG tumor was significantly reduced in the presence of c(RGDyK) in both cases (2.2 ± 0.1 %ID/g vs. 8.6 ± 1.0 %ID/g for ^{64}Cu-DOTA-RGD tetramer and 1.7 ± 0.2 %ID/g vs. 10.6 ± 0.3 %ID/g for ^{64}Cu-DOTA-RGD octamer at 2 h after injection), indicating the in vivo integrin $\alpha_v\beta_3$-binding specificity of both tracers. The uptake of both tracers in all other organs was also significantly lower, similar to that observed for other RGD peptide-based tracers (*33*).

The c-neu oncomouse model has been characterized with radiometal-labeled RGD peptides other than ^{64}Cu. ^{111}In-DOTA-E[c(RGDfK)]$_2$ and ^{90}Y-DOTA-E[c(RGDfK)]$_2$ had, respectively, approximately 3.0 %ID/g at 2 h and approximately 1.5 %ID/g at 24 h after injection, whereas their monomeric counterparts had, respectively, approximately only 1.3 %ID/g at 2 h and approximately only 0.5 %ID/g at 24 h after injection (*34*). Uptake by tumors of our newly developed ^{64}Cu-DOTA-RGD tetramer and ^{64}Cu-DOTA-RGD octamer in this spontaneous mammary carcinoma model was studied. Decay-corrected coronal PET images are shown in Figure 3C, and quantitative data are shown in Figure 4B. Uptake of ^{64}Cu-DOTA-RGD tetramer reached 4.4 ± 0.9 %ID/g (n = 3) at 1 h after injection, with slow clearance (3.6 ± 0.4 %ID/g at 20 h after injection). For ^{64}Cu-DOTA-RGD octamer, uptake was 8.9 ± 2.1 %ID/g (n = 3) at 1 h after injection, almost twice as high as for ^{64}Cu-DOTA-RGD tetramer. Washout from tumor was also slow, with the uptake being 6.6 ± 1.5 %ID/g at 20 h after injection.

Uptake in the liver of oncomice was significantly higher for ^{64}Cu-DOTA-RGD octamer than for ^{64}Cu-DOTA-RGD tetramer. This finding may be attributed to a possible liver metastasis (Fig. 4B). At 7 mo old, all mice had multiple tumors. Because the spontaneous tumor had much higher uptake of ^{64}Cu-DOTA-RGD octamer, the liver metastasis is expected to follow the same trend. Uptake in muscle was similar for both tracers. In the kidney of c-neu oncomice, uptake of ^{64}Cu-DOTA-RGD octamer is also much higher than uptake of ^{64}Cu-DOTA-RGD tetramer, similar to the observation in athymic nude mice.

Biodistribution Studies and Blocking Experiment

To investigate the localization of ^{64}Cu-DOTA-RGD tetramer and ^{64}Cu-DOTA-RGD octamer in normal athymic nude mice, we performed biodistribution studies at 20 h after injection. As can be seen in Figure 5A, uptake of ^{64}Cu-DOTA-RGD tetramer in kidney was 5.0 ± 0.7 %ID/g (n = 3), whereas uptake was almost 5-fold higher for ^{64}Cu-DOTA-RGD octamer (27.0 ± 3.5 %ID/g, n = 3). Because of the slower clearance, uptake of ^{64}Cu-DOTA-RGD octamer was also slightly higher than of ^{64}Cu-DOTA-RGD tetramer in most organs. The biodistribution of ^{64}Cu-DOTA-RGD tetramer in female athymic nude mice with and without a blocking dose of c(RGDyK) is shown in Figure 5B; radioactivity in the kidney and all other dissected tissues was significantly decreased. Quantitative data of the PET scans shown in Figure 3B are presented in Figures 5C and 5D. An excess amount of c(RGDyK) successfully reduced the uptake of both ^{64}Cu-DOTA-RGD tetramer and ^{64}Cu-DOTA-RGD octamer in the U87MG tumor and reduced uptake in the kidney to the background level, confirming the integrin $\alpha_v\beta_3$–binding specificity of both tracers in vivo.

DISCUSSION

This article has described the synthesis of ^{64}Cu-labeled RGD tetramer and RGD octamer based on the RGDyK sequence and their use for PET of tumor integrin $\alpha_v\beta_3$ expression. These RGD multimers showed high integrin

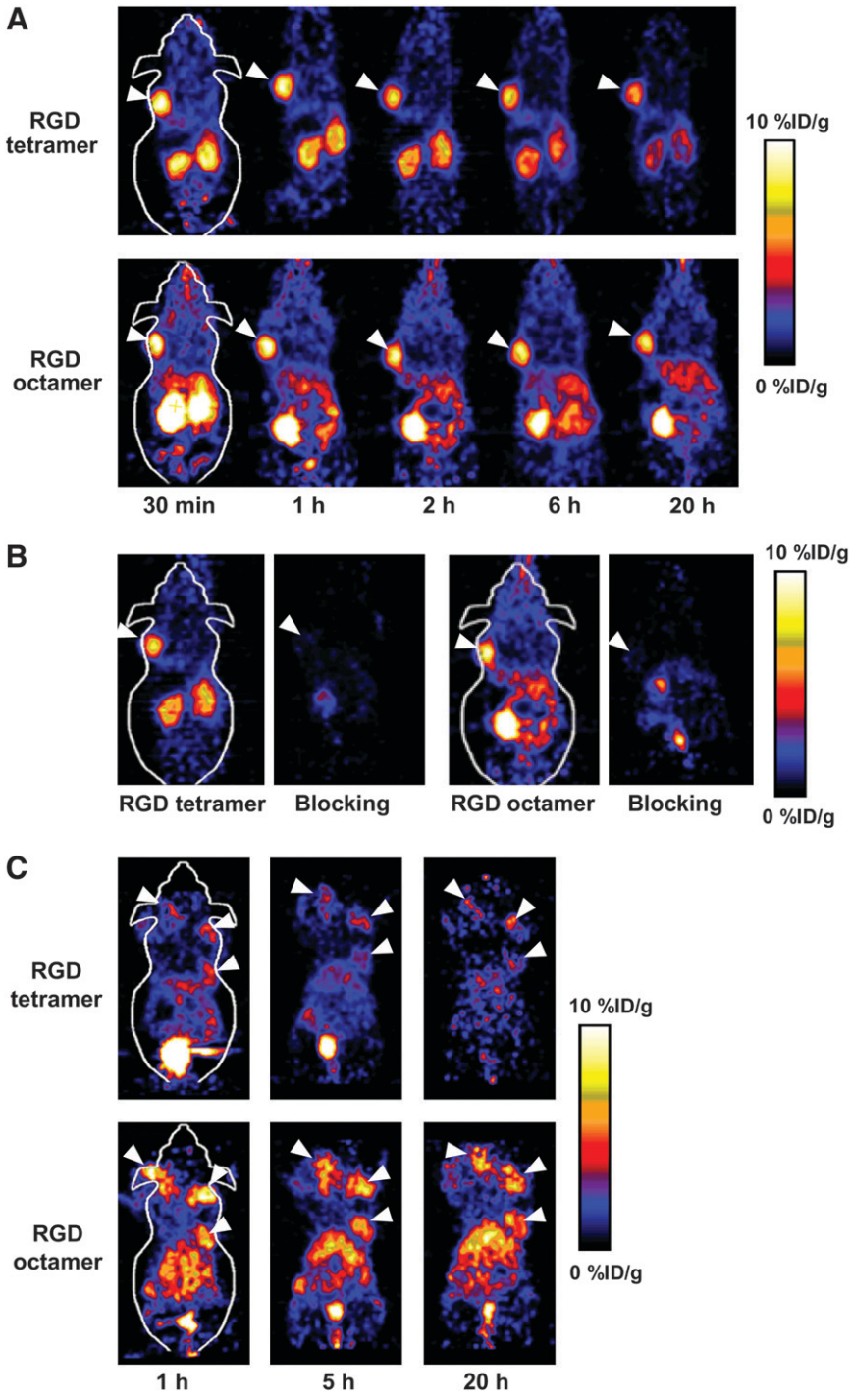

FIGURE 3. Small-animal PET studies of U87MG tumor-bearing mice and c-neu oncomice. (A) Decay-corrected whole-body coronal images of athymic female nude mice bearing U87MG tumor at 30 min and at 1, 2, 6, and 20 h after injection of about 9 MBq of ^{64}Cu-DOTA-RGD tetramer or ^{64}Cu-DOTA-RGD octamer. (B) Coronal images of U87MG tumor-bearing mice at 2 h after injection of ^{64}Cu-DOTA-RGD tetramer or ^{64}Cu-DOTA-RGD octamer without and with (denoted as "blocking") coinjection of 10 mg of c(RGDyK) per kilogram of mouse body weight. (C) Decay-corrected whole-body coronal images of c-neu oncomice at 1, 5, and 20 h after injection of about 9 MBq of ^{64}Cu-DOTA-RGD tetramer or ^{64}Cu-DOTA-RGD octamer. These mice are 7 mo old, and all have multiple tumors. ^{64}Cu-DOTA-RGD tetramer and ^{64}Cu-DOTA-RGD octamer are denoted as "RGD tetramer" and "RGD octamer," respectively. All images shown are of 5- or 10-min static scans and representative of 3 mice per group. Tumors are indicated by arrows.

$\alpha_v\beta_3$-binding affinity and specificity as determined by a cell adhesion assay and a cell-binding assay. The binding affinity and specificity of the newly developed tracers (^{64}Cu-DOTA-RGD tetramer and ^{64}Cu-DOTA-RGD octamer) in vivo was also confirmed by biodistribution studies and quantitative small-animal PET experiments.

A variety of radiolabeled peptides has been evaluated for tumor localization and therapy (*15,16,20,21,23,32,35*). Radiolabeled RGD peptides are of particular interest because they bind to integrin $\alpha_v\beta_3$, which is overexpressed on newly formed blood vessels and the cells of many common cancer types. However, most RGD peptide-based tracers developed so far have fast blood clearance accompanied by relatively low tumor uptake and rapid tumor washout, presumably because of the suboptimal receptor-binding affinity/selectivity and inadequate contact with the binding pocket located in the extracellular segment of integrin $\alpha_v\beta_3$.

We and others have previously applied the concept of bivalency to develop dimeric RGD peptides for tumor targeting (*13,23,32,35,36*). The introduction of the dimeric

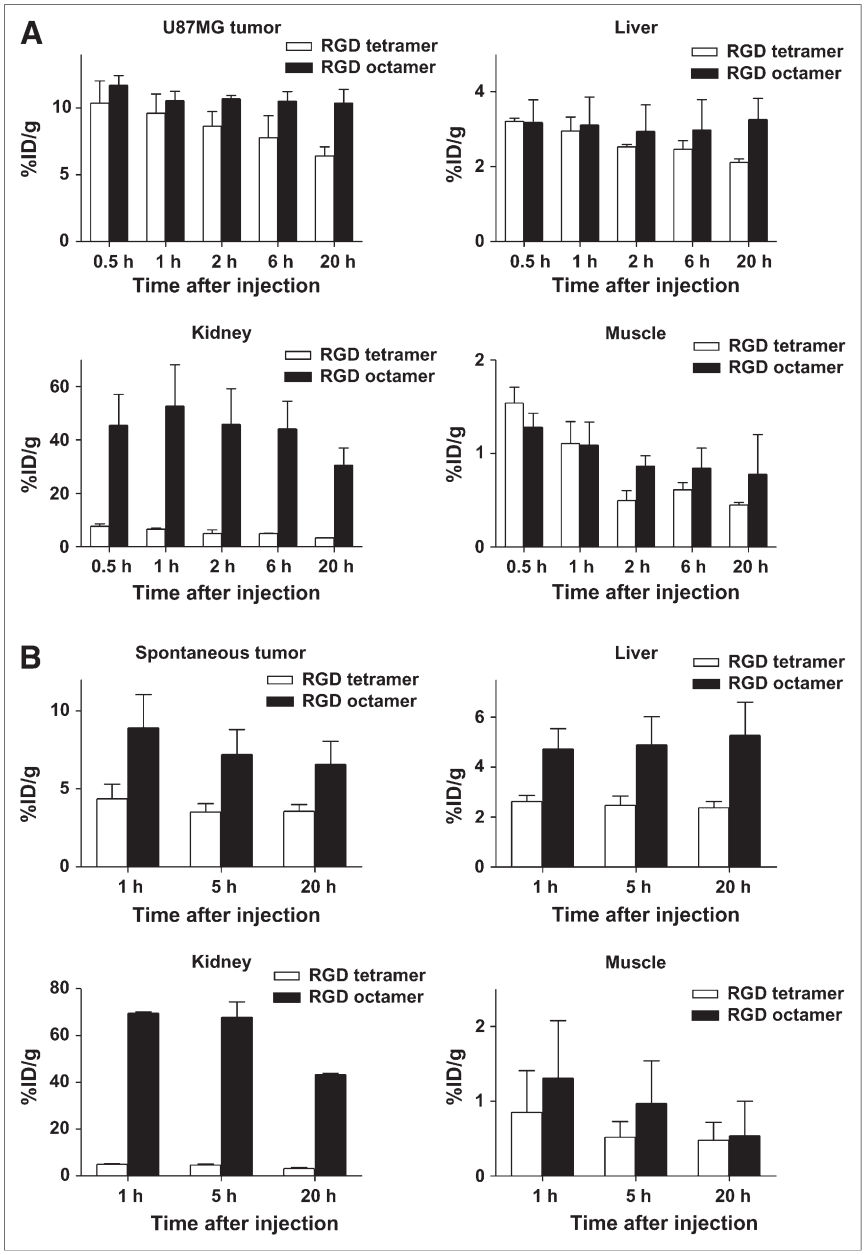

FIGURE 4. Quantitative analyses of small-animal PET data. (A) Comparison between ^{64}Cu-DOTA-RGD tetramer and ^{64}Cu-DOTA-RGD octamer uptake in U87MG tumor, liver, kidney, and muscle over time in U87MG xenograft model (n = 3). (B) Comparison between ^{64}Cu-DOTA-RGD tetramer and ^{64}Cu-DOTA-RGD octamer uptake in spontaneous tumor, liver, kidney, and muscle over time in c-neu oncomice (n = 3).

RGD peptide system resulted in increased receptor-binding affinity/specificity for integrin $\alpha_v\beta_3$ in vitro and enhanced tumor uptake and retention in vivo, compared with those of RGD monomer. Recently, we reported that ^{64}Cu-labeled tetrameric RGDfK peptide had significantly higher affinity and specificity than either RGD dimer or RGD monomer in the integrin $\alpha_v\beta_3$-positive U87MG tumor model because of the synergistic effect of polyvalency (*20*). Previously, we also found that replacing D-Phe (f) with D-Tyr (y) increased the hydrophilicity of the RGD peptides and resulted in increased integrin $\alpha_v\beta_3$-mediated tumor uptake and more favorable biokinetics in an orthotopic MDA-MB-435 breast cancer model (*32*). On the basis of these findings and an incremental improvement in tumor targeting and pharmacokinetics, compared with the previous RGD peptide analogs, we then devoted our efforts to the synthesis of tetrameric and octameric RGD peptides with repeating c(RGDyK) units connected through glutamate linkers.

With the RGD/integrin system, polyvalency has been shown to be able to significantly improve integrin-binding affinity and selectivity (*22*). The minimum linker length between the 2 RGD moieties has been reported to be about 3.5 nm (~25 bond distances) for simultaneous integrin $\alpha_v\beta_3$-binding in the immobilized integrin $\alpha_v\beta_3$ assay (*37*). For our RGD tetramer $(E\{E[c(RGDyK)]_2\}_2$ (Fig. 1A), the longest distance between the 2 RGD motifs is about 30 bond lengths, long enough for simultaneous binding to adjacent integrin $\alpha_v\beta_3$. For RGD octamer, the distance is about 40 bond lengths, and simultaneous binding to 2 or more receptors is possible.

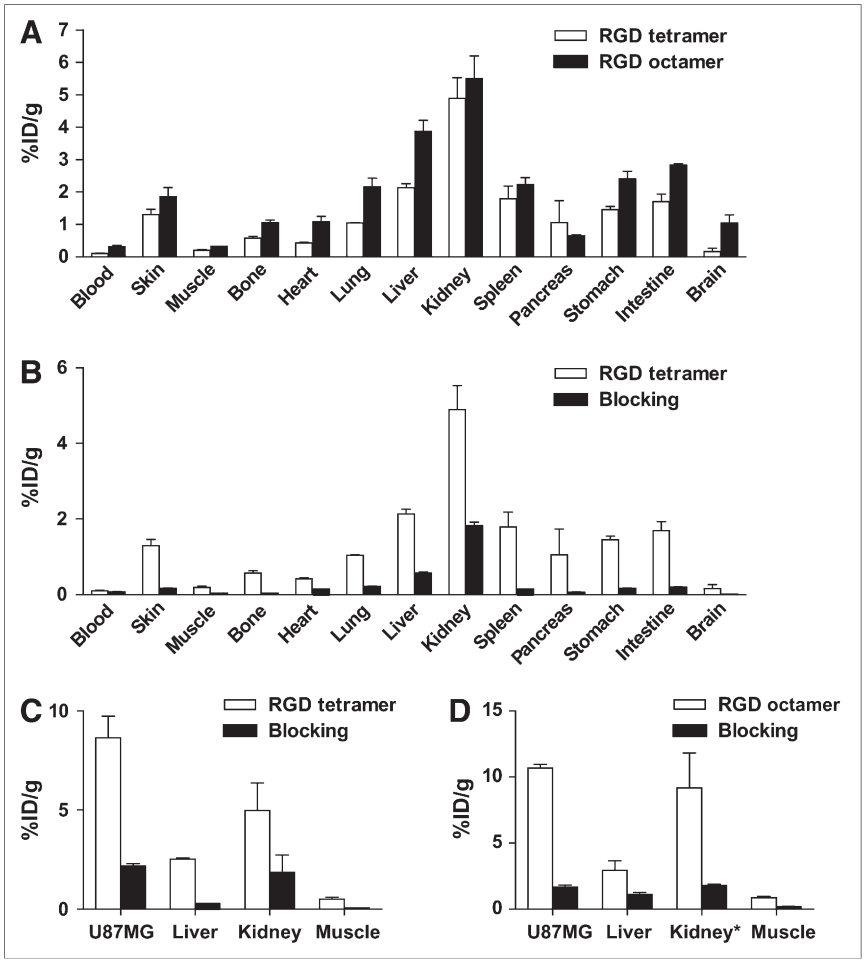

FIGURE 5. Biodistribution and receptor blocking experiments. (A) Biodistribution of ^{64}Cu-DOTA-RGD tetramer and ^{64}Cu-DOTA-RGD octamer in female athymic nude mice at 20 h after injection (n = 3). Plotted kidney uptake of ^{64}Cu-DOTA-RGD octamer is one fifth of actual value (*). (B) Biodistribution of ^{64}Cu-DOTA-RGD tetramer in female athymic nude mice at 20 h after injection with and without coinjection of 10 mg of c(RGDyK) per kilogram (n = 3). (C) Comparison of ^{64}Cu-DOTA-RGD tetramer uptake at 2 h after injection in U87MG tumor, kidneys, liver, and muscle over time with and without coinjection of 10 mg of c(RGDyK) per kilogram (n = 3). (D) Comparison of ^{64}Cu-DOTA-RGD octamer uptake in U87MG tumor, kidneys, liver, and muscle over time with and without coinjection of 10 mg of c(RGDyK) per kilogram (n = 3). Plotted kidney uptake of ^{64}Cu-DOTA-RGD octamer is one fifth of actual value (*).

We used 2 types of assays to examine the interaction between RGD multimers and $\alpha_v\beta_3$ integrin. We first used a cell adhesion assay to assess the antiadhesion effect of RGD multimers against integrin $\alpha_v\beta_3$. RGD octamer showed a significantly better inhibition ability than the monomer/dimer/tetramer counterparts, as could be attributed to the multiple binding sites or significantly increased local concentration. To evaluate the effect of polyvalency, we calculated the multivalent enhancement ratio (MVE), which was obtained by dividing the IC_{50} value for the RGD monomer by the IC_{50} of the RGD multimer (*27*). The antiadhesion MVE of RGD tetramer and RGD octamer was 8.4 and 25.6, respectively (Table 1). We then performed a cell-binding assay, an often-used method to determine the receptor-binding affinity of a given ligand. Again, the integrin $\alpha_v\beta_3$-binding affinity followed the order of RGD octamer > RGD tetramer > RGD dimer > RGD monomer (Fig. 2C; Table 1). DOTA conjugation had a minimal effect on the binding affinity of the RGD peptides. The receptor-binding MVE for RGD tetramer and RGD octamer was calculated to be 5.9 and 20.3, respectively. On the basis of both the cell adhesion assay and the cell-binding assay, RGD octamer showed a stronger multivalent effect than did RGD tetramer.

When applied to the U87MG glioblastoma xenograft model, which has been well established to have a high integrin $\alpha_v\beta_3$ expression (*20,38*), ^{64}Cu-DOTA-RGD tetramer showed prominent uptake in tumor and primarily renal clearance (Figs. 3A and 4A). ^{64}Cu-DOTA-RGD octamer had slightly higher initial tumor uptake and much longer tumor retention. The initially rapid and high tumor uptake might be attributed to the high integrin $\alpha_v\beta_3$-binding affinity of both tracers. The larger molecular size of ^{64}Cu-DOTA-RGD octamer, along with the stronger MVE, may be attributed to its longer circulation time and slower tumor washout, compared with those of ^{64}Cu-DOTA-RGD tetramer. We also tested these 2 tracers in the c-neu oncomouse model. Both tracers showed significantly higher uptake in the spontaneous tumor (medium integrin expression) than did the dimeric and monomeric analogs. The difference between ^{64}Cu-DOTA-RGD tetramer and ^{64}Cu-DOTA-RGD octamer is more substantial in this model than in the U87MG xenograft model. Uptake of ^{64}Cu-DOTA-RGD octamer in tumor was almost twice as high as uptake of ^{64}Cu-DOTA-RGD tetramer (Fig. 4B). A similar pattern has also been observed in the orthotopic MDA-MB-435 (medium integrin expression) breast cancer model. The advantage of higher integrin $\alpha_v\beta_3$-binding

TABLE 1
MVE of RGD Multimers Based on Cell Adhesion and Cell-Binding Assays Using Human Glioblastoma U87MG Cells

Parameter	RGD monomer	RGD dimer	RGD tetramer	RGD octamer
Antiadhesion IC_{50} (nmol/L)	2,710 ± 720	695 ± 99	323 ± 85	106 ± 22
Antiadhesion MVE	1	3.9	8.4	25.6
Cell binding IC_{50} (nmol/L)	203 ± 32	103 ± 14	34.6 ± 2.6	10.0 ± 1.7
Cell binding MVE	1	1.97	5.87	20.3

Concentrations are expressed as mean ± SD (n = 3), and MVE is IC_{50} of RGD monomer divided by IC_{50} of RGD multimers.

affinity and selectivity of RGD octamer over RGD tetramer appears to be more obvious in medium integrin $\alpha_v\beta_3$-expressing tumor models (e.g., MDA-MB-435 and c-neu oncomice) than in high integrin-expressing tumor models (e.g., U87MG). The mechanism underlying such a phenomenon remains to be elucidated.

Compared with ^{64}Cu-DOTA-RGD tetramer, ^{64}Cu-DOTA-RGD octamer exhibited significantly higher renal uptake in both subcutaneous U87MG xenografts and mammary adenocarcinoma–bearing c-neu oncomice. We initially proposed that the high renal uptake of ^{64}Cu-DOTA-RGD octamer, compared with other RGD oligomers, might be caused by the overall difference in molecular charge. If we assign a value of −1 to each acidic residue (Asp (D) and Glu (E)) and the C-terminal -COOH, and a value of +1 to each basic residue (Arg (R) and Lys (K)) and the N-terminal -NH_2, the overall charge of the peptide can be determined by adding up the charges. For both RGD tetramer and RGD octamer, the overall molecular charges are +1 although RGD octamer has a higher number of charged amino acid residues. Positively charged radiolabeled peptides or metabolites are usually retained in the kidney after resorption by renal tubular cells and lysosomal proteolysis. Blocking cationic binding sites in the kidneys with cationic amino acid infusion has been reported to reduce renal uptake without compromising the accumulation of activity in the tumor in both mice and humans (*39*). We tried the blocking experiment for ^{64}Cu-DOTA-RGD octamer by coinjecting an excess amount of D-lysine; uptake in the kidney was only marginally reduced, suggesting that the overall molecular charge does not contribute significantly to the high renal uptake.

We noticed that even though uptake of ^{64}Cu-DOTA-RGD octamer in the kidney was high, no appreciable activity was excreted to the urinary bladder over time. Such a phenomenon suggests that receptor-mediated binding might be involved. Integrins play important roles in renal development, and integrin $\alpha_v\beta_3$, in particular, has been identified in many parts of the developing kidney. Integrin $\alpha_v\beta_3$ is expressed in the renal endothelium of adults and, to a lesser extent, in all tubular epithelium (*40*). Effective blocking of activity accumulation in the kidney in the presence of an excess amount of c(RGDyK) also confirmed the integrin $\alpha_v\beta_3$ specificity of both ^{64}Cu-DOTA-RGD tetramer and ^{64}Cu-DOTA-RGD octamer (Figs. 2B and 5B). Immunohistochemical staining showed that mouse kidneys have high β_3 expression on the endothelial cells of small glomerulus vessels (Supplemental Fig. 2), further confirming that renal uptake of both tracers is integrin-specific. The trend of increased kidney uptake from RGD monomer to dimer to tetramer to octamer would thus be due, in part, to the increased $\alpha_v\beta_3$-binding affinity and the molecular size.

It is important to have high tumor-to-kidney ratios, as well as high absolute tumor uptake and longer retention, for both imaging and therapeutic applications. For imaging purposes, renal accumulation of radiolabeled peptides will reduce detection sensitivity in the vicinity of the kidneys. For therapeutic applications, renal accumulation of radiolabeled peptides limits the maximum tolerated doses that can be administered without inducing radiation nephrotoxicity. Thus, further modification is needed to improve the pharmacokinetics of RGD peptide-based radiopharmaceuticals. First, high $\alpha_v\beta_3$-binding affinity is needed to afford high uptake and retention in tumors. For RGD octamer, the density of RGD units is rather high, and not all RGD units are amenable to effective binding to integrin $\alpha_v\beta_3$ located on the same cell surface. Our future work will focus on the structure–activity relationship to develop various dendritic and polymeric scaffolds for attaching RGD peptides, thereby further enhancing the multivalency effect. Second, appropriate modification of the DOTA-RGD multimers is needed to reduce renal uptake. By inserting a bifunctional linker between the DOTA chelator and the RGD multimer as a pharmacokinetic modifier, we may be able to modulate the overall molecular charge, hydrophilicity, and molecular size, thus possibly improving in vivo pharmacokinetics without compromising the tumor-targeting efficacy of the resulting radioconjugates.

CONCLUSION

^{64}Cu-DOTA-RGD tetramer and ^{64}Cu-DOTA-RGD octamer were developed for PET of tumor integrin $\alpha_v\beta_3$ expression. RGD octamer showed significantly higher integrin $\alpha_v\beta_3$-binding affinity in vitro than did RGD tetramer. In the noninvasive small-animal PET studies, both tracers showed rapid and high uptake in tumor, slow washout, and good tumor-to-background contrast in U87MG xenografts and c-neu oncomice. Overall, polyvalency has a profound

effect on the receptor-binding affinity and in vivo kinetics of ^{64}Cu-DOTA-RGD multimers. The information obtained here may guide future development of integrin $\alpha_v\beta_3$-targeted imaging and internal radiotherapy agents. These RGD peptide-based radiopharmaceuticals may also have promising applications in other angiogenesis-related diseases such as rheumatoid arthritis, myocardial infarction, and stroke.

ACKNOWLEDGMENTS

This work was supported by the National Institute of Biomedical Imaging and Bioengineering (R21 EB001785), the National Cancer Institute (R21 CA102123, P50 CA114747, U54 CA119367, and R24 CA93862), the Department of Defense (W81XWH-04-1-0697, W81XWH-06-1-0665, W81XWH-06-1-0042, and DAMD17-03-1-0143), and a Benedict Cassen Postdoctoral Fellowship from the Education and Research Foundation of the Society of Nuclear Medicine. We thank Dr. Hui Wang and Dr. Gang Niu for their excellent technical support. We also thank the cyclotron team at the University of Wisconsin–Madison, for ^{64}Cu production.

REFERENCES

1. Brooks PC, Clark RA, Cheresh DA. Requirement of vascular integrin $\alpha_v\beta_3$ angiogenesis. *Science.* 1994;264:569–571.
2. Polverini PJ. Angiogenesis in health and disease: insights into basic mechanisms and therapeutic opportunities. *J Dent Educ.* 2002;66:962–975.
3. Folkman J. Angiogenesis in cancer, vascular, rheumatoid and other disease. *Nat Med.* 1995;1:27–31.
4. Shahan T, Grant D, Tootell M, et al. Oncothanin, a peptide from the α_3 chain of type IV collagen, modifies endothelial cell function and inhibits angiogenesis. *Connect Tissue Res.* 2004;45:151–163.
5. Puduvalli VK. Inhibition of angiogenesis as a therapeutic strategy against brain tumors. *Cancer Treat Res.* 2004;117:307–336.
6. Sengupta S, Chattopadhyay N, Mitra A, Ray S, Dasgupta S, Chatterjee A. Role of $\alpha_v\beta_3$ integrin receptors in breast tumor. *J Exp Clin Cancer Res.* 2001;20:585–590.
7. Friedlander M, Brooks PC, Shaffer RW, Kincaid CM, Varner JA, Cheresh DA. Definition of two angiogenic pathways by distinct α_v integrins. *Science.* 1995; 270:1500–1502.
8. Horton MA. The $\alpha_v\beta_3$ integrin "vitronectin receptor." *Int J Biochem Cell Biol.* 1997;29:721–725.
9. Bello L, Francolini M, Marthyn P, et al. $\alpha_v\beta_3$ and $\alpha_v\beta_5$ integrin expression in glioma periphery discussion 390. *Neurosurgery.* 2001;49:380–389.
10. Jin H, Varner J. Integrins: roles in cancer development and as treatment targets. *Br J Cancer.* 2004;90:561–565.
11. Kumar CC. Integrin $\alpha_v\beta_3$ as a therapeutic target for blocking tumor-induced angiogenesis. *Curr Drug Targets.* 2003;4:123–131.
12. Jung KH, Lee KH, Paik JY, et al. Favorable biokinetic and tumor-targeting properties of ^{99m}Tc-labeled glucosamino RGD and effect of paclitaxel therapy. *J Nucl Med.* 2006;47:2000–2007.
13. Zhang X, Xiong Z, Wu Y, et al. Quantitative PET imaging of tumor integrin $\alpha_v\beta_3$ expression with ^{18}F-FRGD$_2$. *J Nucl Med.* 2006;47:113–121.
14. Tucker GC. α_v integrin inhibitors and cancer therapy. *Curr Opin Investig Drugs.* 2003;4:722–731.
15. Dijkgraaf I, Kruijtzer JA, Liu S, et al. Improved targeting of the $\alpha_v\beta_3$ integrin by multimerisation of RGD peptides. *Eur J Nucl Med Mol Imaging.* 2007;34:267–273.
16. Dijkgraaf I, Liu S, Kruijtzer JA, et al. Effects of linker variation on the in vitro and in vivo characteristics of an ^{111}In-labeled RGD peptide. *Nucl Med Biol.* 2007;34:29–35.
17. Beer AJ, Haubner R, Goebel M, et al. Biodistribution and pharmacokinetics of the $\alpha_v\beta_3$-selective tracer ^{18}F-galacto-RGD in cancer patients. *J Nucl Med.* 2005; 46:1333–1341.
18. Sharma SD, Jiang J, Hadley ME, Bentley DL, Hruby VJ. Melanotropic peptide-conjugated beads for microscopic visualization and characterization of melanoma melanotropin receptors. *Proc Natl Acad Sci U S A.* 1996;93:13715–13720.
19. Mammen M, Chio S-K, Whitesides GM. Polyvalent interactions in biological systems: implications for design and use of multivalent ligands and inhibitors. *Angew Chem Int Ed Engl.* 1998;37:2755–2794.
20. Wu Y, Zhang X, Xiong Z, et al. microPET imaging of glioma integrin $\alpha_v\beta_3$ expression using ^{64}Cu-labeled tetrameric RGD peptide. *J Nucl Med.* 2005;46: 1707–1718.
21. Liu S. Radiolabeled multimeric cyclic RGD peptides as integrin $\alpha_v\beta_3$ targeted radiotracers for tumor imaging. *Mol Pharm.* 2006;3:472–487.
22. Ye Y, Bloch S, Xu B, Achilefu S. Design, synthesis, and evaluation of near infrared fluorescent multimeric RGD peptides for targeting tumors. *J Med Chem.* 2006;49:2268–2275.
23. Liu S, Edwards DS, Ziegler MC, Harris AR, Hemingway SJ, Barrett JA. ^{99m}Tc-labeling of a hydrazinonicotinamide-conjugated vitronectin receptor antagonist useful for imaging tumors. *Bioconjug Chem.* 2001;12:624–629.
24. Thumshirn G, Hersel U, Goodman SL, Kessler H. Multimeric cyclic RGD peptides as potential tools for tumor targeting: solid-phase peptide synthesis and chemoselective oxime ligation. *Chem Eur J.* 2003;9:2717–2725.
25. Boturyn D, Coll J-L, Garanger E, Favrot M-C, Dumy P. Template assembled cyclopeptides as multimeric system for integrin targeting and endocytosis. *J Am Chem Soc.* 2004;126:5730–5739.
26. Dirksen A, Langereis S, de Waal BFM, van Genderen MHP, Hackeng TM, Meijer EW. A supramolecular approach to multivalent target-specific MRI contrast agents for angiogenesis. *Chem Commun (Camb).* 2005;2811–2813.
27. Montet X, Funovics M, Montet-Abou K, Weissleder R, Josephson L. Multivalent effects of RGD peptides obtained by nanoparticle display. *J Med Chem.* 2006;49: 6087–6093.
28. Muller WJ, Sinn E, Pattengale PK, Wallace R, Leder P. Single-step induction of mammary adenocarcinoma in transgenic mice bearing the activated c-neu oncogene. *Cell.* 1988;54:105–115.
29. Ruoslahti E. RGD and other recognition sequences for integrins. *Annu Rev Cell Dev Biol.* 1996;12:697–715.
30. Ogata T, Teshima T, Kagawa K, et al. Particle irradiation suppresses metastatic potential of cancer cells. *Cancer Res.* 2005;65:113–120.
31. Haubner R, Wester HJ, Burkhart F, et al. Glycosylated RGD-containing peptides: tracer for tumor targeting and angiogenesis imaging with improved biokinetics. *J Nucl Med.* 2001;42:326–336.
32. Chen X, Liu S, Hou Y, et al. microPET imaging of breast cancer α_v-integrin expression with ^{64}Cu-labeled dimeric RGD peptides. *Mol Imaging Biol.* 2004;6: 350–359.
33. Cai W, Zhang X, Wu Y, Chen X. A thiol-reactive ^{18}F-labeling agent, N-[2-(4-^{18}F-fluorobenzamido)ethyl]maleimide, and synthesis of RGD peptide-based tracer for PET imaging of $\alpha_v\beta_3$ integrin expression. *J Nucl Med.* 2006;47: 1172–1180.
34. Liu S, Robinson SP, Edwards DS. Radiolabeled integrin $\alpha_v\beta_3$ antagonists as radiopharmaceuticals for tumor radiotherapy. *Top Curr Chem.* 2005;252:193–216.
35. Janssen ML, Oyen WJ, Dijkgraaf I, et al. Tumor targeting with radiolabeled $\alpha_v\beta_3$ integrin binding peptides in a nude mouse model. *Cancer Res.* 2002;62:6146–6151.
36. Janssen M, Frielink C, Dijkgraaf I, et al. Improved tumor targeting of radiolabeled RGD peptides using rapid dose fractionation. *Cancer Biother Radiopharm.* 2004;19:399–404.
37. Poethko T, Schottelius M, Thumshirn G, et al. Chemoselective pre-conjugate radiohalogenation of unprotected mono- and multimeric peptides via oxime formation. *Radiochimica Acta.* 2004;92:317–327.
38. Zhang X, Xiong Z, Wu Y, et al. Quantitative PET imaging of tumor integrin $\alpha_v\beta_3$ expression with ^{18}F-FRGD$_2$. *J Nucl Med.* 2006;47:113–121.
39. van Eerd JEM, Vegt E, Wetzels JFM, et al. Gelatin-based plasma expander effectively reduces renal uptake of ^{111}In-octreotide in mice and rats. *J Nucl Med.* 2006;47:528–533.
40. Hamerski DA, Santoro SA. Integrins and the kidney: biology and pathobiology. *Curr Opin Nephrol Hypertens.* 1999;8:9–14.